Lasers in Manufacturing Conference 2021

Analytical approach for the transition to an equiaxed dendritic solidification during laser beam welding of aluminium alloys

Constantin Böhm[a,*], Yassin Nasr[a], Jonas Wagner[b], Christian Hagenlocher[b], Stefan Weihe[a]

[a]*University of Stuttgart, Materials Testing Institute (MPA), Pfaffenwaldeing 32, D-70569 Stuttgart, Germany*
[b]*University of Stuttgart, Institut für Strahlwerkzeuge (IFSW), Pfaffenwaldring 43, D-70569 Stuttgart, Germany*

Abstract

An equiaxed solidification in a laser beam welded seam is beneficial. It leads to grain refinement, which increases mechanical strength and hot cracking resistance. The effects of filler wire addition and welding parameters on the resulting grain structure are experimentally well studied. Up until now, there has been no description of the process window for equiaxed solidification in terms of the process parameters. This work presents an analytical approach to access the description of the columnar-to-equiaxed transition based on fundamental solidification theory for a wide-range of aluminium alloys and laser welding parameters. To validate the approach, the theoretically calculated powers are compared to experimental results of full-penetrated weld seams. This study provides an overview of the key process parameters and the material characteristics, which determine the solidification mode – in this case columnar or equiaxed dendritic. Furthermore, a process window for grain refinement of aluminium alloys is derived.

Keywords: aluminium alloys; laser beam welding; grain structure; equiaxed solidification; grain refinement

1. Introduction

In welding of aluminium alloys hot cracks are severe defects. Tang and Vollertsen, 2014, Hagenlocher et al., 2019b and Schempp and Rethmeier, 2015 showed that an equiaxed grain structure and grain refinement improve the hot cracking resistance of the weld seam and can even lead to hot crack free weld seams.

* Corresponding author. Tel.: +49-711-685-60774 .
E-mail address: constantin.boehm@mpa.uni-stuttgart.de .

Therefore, it is important to understand how the process parameters and the alloy composition influence the equiaxed dendritic solidification and the grain size.

In remote laser beam welding of aluminium alloys the weld grain structure can be altered by different process parameters. Fig. 1 depicts the surface parallel micrograph of a weld seam with (a) fully columnar dendritic grain structure and (b) an equiaxed dendritic grain structure in the weld centre. In Fig. 1(b) the equiaxed dendritic grain structure leads to a grain refinement and hence a higher hot cracking resistance.

Böhm et al., 2021 derived in a previous work an analytical description of the criterion for the columnar-to-equiaxed transition (CET) during laser beam welding of aluminium alloys that highlighted the influence of the process parameter on the equiaxed dendritic solidification. Up to now, the influence of the aluminium alloy composition on the equiaxed dendritic solidification is unknown. Therefore, in this study weld experiments were conducted on the alloys EN AW-7075, EN AW-6016, EN AW-5754, EN AW-5083 and EN AW-2024. Additionally, the influence of the cooling rate on the equiaxed dendritic grain size is highlighted.

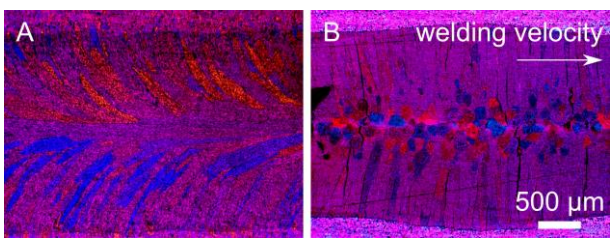

Fig. 1. Optical micrographs of a surface parallel cross section viewed under polarized light show different dendritic grain structure in the weld seam of EN AW-6016 for different process parameters. (a) laser power P = 620 W, welding velocity v = 0.25 m/min, focal diameter d_f = 50 µm with a full penetration depth of 2.4 mm. (b) laser power P = 6000 W, welding velocity v = 12 m/min, focal diameter d_f = 560 µm with a full penetration depth of 2 mm, Böhm et al., 2021 (CC BY 4.0).

2. Analytical approach: Criterion for columnar-to-equiaxed transition

This section summarizes the theoretical background in order to calculate the process parameters to reach a beneficial equiaxed dendritic solidification. In a prior study, Böhm et al., 2021 presented the criterion for the columnar-to-equiaxed transition during laser beam welding. The analytical description combines a special solution of the 2D heat flux in full penetration laser beam welding presented by Hagenlocher et al., 2019a based on Rosenthal, 1941 with the criterion for columnar-to-equiaxed transition of Hunt, 1984 and basics of nucleation theory Dantzig and Rappaz, 2016. The interested reader is referred to Böhm et al., 2021 for the detailed derivation of the following equations (1) and (2).

The required absorbed power per unit depth that leads to an equiaxed solidification is described as

$$P_{\mathrm{depth,req}} \cdot \eta_{\mathrm{abs}} = 6.75 \cdot \left(\frac{1}{N_{\mathrm{active}}}\right)^{\frac{1}{6}} \cdot v^{\frac{1}{4}} \cdot \xi^{\frac{1}{2}} \qquad (1)$$

where η_{abs} is the absorptance, N_{active} is the active nucleation density, v is the welding velocity and

$$\xi = \frac{\left(T_{\mathrm{liq}} - T_{\mathrm{amb}}\right)^3 \cdot \lambda_{\mathrm{th}} \cdot \rho_s \cdot c_p}{A_i} \qquad (2)$$

is the extended alloy parameter which is described by the liquidus temperature T_{liq}, the ambient temperature of the work piece T_{amb}, the heat conductivity λ_{th}, the solid density ρ_s, the heat capacity c_p and the undercooling parameter A_i. Eq. (2) summarizes the influence of the alloy on the required power per unit depth. The extended alloy parameter has a minimum and maximum value due to the range of the alloy composition according to DIN EN 573-3.

The exact distribution of the nucleation particles in commercially available aluminium alloys is unknown. Böhm et al., 2021 found that the active nucleation density is in the range of $N_{active} = 10^{11} – 10^{13}$ 1/m³ for two different alloy batches of EN AW-6016 and a wide range of laser beam welding parameters. Therefore, we assume that for wrought aluminium alloys the active nucleation density is between $N_{active,min} = 10^{11}$ 1/m³ and $N_{active,max} = 10^{13}$ 1/m³. This leads to a minimum and maximum value for the absorbed power per unit depth that is required for an equiaxed dendritic solidification:

$$P_{depth,req,min} \cdot \eta_{abs} \approx 0.05 \cdot v^{\frac{1}{4}} \cdot \xi_{min}^{\frac{1}{2}} \text{ ; for } N_{active} = N_{max}, \quad (3)$$

$$P_{depth,req,max} \cdot \eta_{abs} \approx 0.1 \cdot v^{\frac{1}{4}} \cdot \xi_{max}^{\frac{1}{2}} \text{; for } N_{active} = N_{min} . \quad (4)$$

It is expected that for all absorbed power per unit depths greater than the minimum value according to Eq. (3) equiaxed dendritic solidification occurs.

The required thermo-physical properties for the equations (3) and (4) were calculated by Thermo-Calc 2020a with the aluminium database v5.1 Andersson et al., 2002 and are listed in Table 1. The detailed calculation procedure is presented by Böhm et al., 2021.

Table 1. List of thermo-physical properties calculated according to Böhm et al., 2021.

Alloy designation DIN EN 573-3	A_I (Ks$^{0.5}$/mm$^{0.5}$)		N_{active} (1/m³)		ξ (10^{15} J²/s$^{1.5}$m$^{3.5}$)	
	Min	Max	Min	Max	Min	Max
EN AW-7075 (Al Zn5.5MgCu)	38.2	68.1			1.161	2.237
EN AW-6016 (Al Si1.2Mg0.4)	104.1	140.9			0.756	1.169
EN AW-5083 (Al Mg4.5Mn0.7)	54.7	110.7	10^{11}	10^{13}	1.517	2.921
EN AW-5754 (Al Mg3)	84.8	108.6			0.741	0.954
EN AW-2024 (Al Cu4Mg1)	133.9	166.7			0.457	0.581

3. Material and Method

The weld experiments were conducted with two disk lasers. A TRUMPF TruDisk 16002 and a TRUMPF TruDisk 8001. Both operate at a wavelength of λ = 1.03 µm. The processing optics were inclined opposite to the welding direction by 12°. The laser beam power was adjusted to reach keyhole mode welding and fully penetrated sheets for different sheet thicknesses t_{sheet} = 2 mm and 4 mm welding velocities v = 0.5 – 6 m/min and focal diameters d_f = 50 – 1500 µm. Furthermore, the laser beam power was adjusted to reach values lower and greater than the values calculated by Eq. (3) and (4). The absorptance was calculated for a cylindrically

capillary according to Gouffé, 1945 with minor corrections from Hügel and Graf, 2014 with an absorptivity of liquid aluminum of 0.15 and a capillary depth equal to the sheet thickness.

The welded samples were grinded and polished mechanically. The polished surfaces were etched anodically with Barker's reagent. The etched samples were analysed by means of an optical microscope with polarized illumination to reveal the grain structure. The size of the equiaxed dendritic grains was determined with the line intercept method with a line length of 2 mm according to DIN EN ISO 643. The grain size was measured in the weld centreline. The measurement was repeated three times and the minimum, mean and maximum grain size was calculated.

4. Results

4.1. Comparing analytical approach with experimental results

According to Eq. (1) the type of grain structure (equiaxed or columnar dendritic) can be predicted. This section compares the experimental results and with the predictions of the analytical approach. The results of EN AW-7075, EN AW-6016 and EN AW-5083 are representatives for all the researched alloys and their results are presented and discussed in the following.

Fig. 2, Fig. 3 and Fig. 4 show the required absorbed power per unit depth that leads to an equiaxed solidification as a function of the welding velocity. The lower green curve represents the minimum required power per unit depth according to Eq. (3). Experimental data points lower than the green curve are expected to have a fully columnar dendritic grain structure in the weld seam as depicted in in Fig. 1a. The upper purple curve represents the maximum required power per depth according to Eq. (4). Experimental data points higher than the purple curve are expected to have fully equiaxed dendritic structure in the weld seam centre as depicted in in Fig. 1b. The points indicate experimental data and are colour coded according to the grain structure of the weld seam: a fully filled white data point represents a fully columnar grain structure, half-filled blue and white represents a transition behaviour and a fully filled blue represents a fully equiaxed grain structure. The error bars represent the uncertainty in the calculation of the absorbed power per unit depth by ± 10 % of the calculated value. For each alloy, two representative micrographs of the grain structure are given next to the graphs.

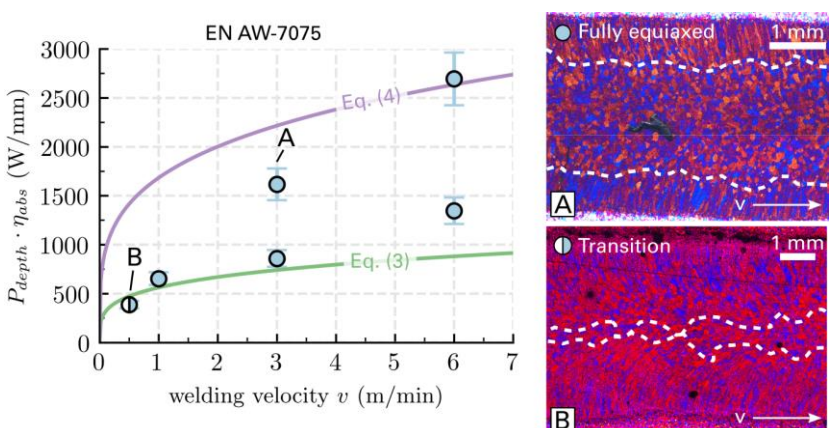

Fig. 2. Experimental results of EN AW-7075 are depicted for different absorbed power per unit depths and welding velocities. A half-filled circle indicates a transition behaviour between columnar and equiaxed dendritic grains and a circle filled with blue indicates a fully equiaxed dendritic grain structure in the weld centre. The green and purple lines are calculated by Eq. (3) and Eq. (4). They represent the expected minimum and maximum value for columnar to equiaxed transition.

Fig. 2 depicts the experimental results of EN AW-7075. In EN AW-7075 the experimental results show an equiaxed dendritic grain structure as soon as the minimum values for the absorbed power per unit depth (green curve) according to Eq. (3) are surpassed. A transition behaviour between columnar and equiaxed dendritic grains in the weld centre is observed for the velocity of v = 0.5 m/min.

Fig. 3 depicts the experimental results of EN AW-6016. The experimental results show an equiaxed dendritic grain structure as soon as the minimum values for the absorbed power per unit depth (green curve) according to Eq. (3) are surpassed. A transition behaviour between columnar and equiaxed dendritic grains in the weld centre is observed for the velocity of v = 1 m/min.

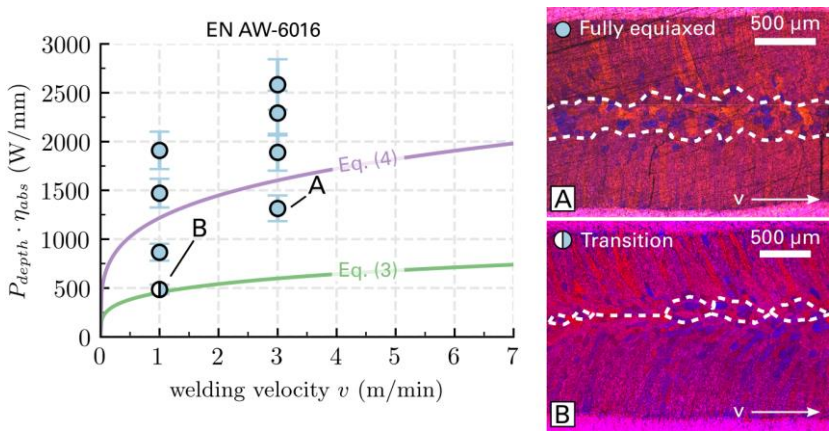

Fig. 3. Experimental results of EN AW-6016 are depicted for different absorbed power per unit depths and welding velocities. A half-filled circle indicates a transition behaviour between columnar and equiaxed dendritic grains and a circle filled with blue indicates a fully equiaxed dendritic grain structure in the weld centre. The green and purple lines are calculated by Eq. (3) and Eq. (4). They represent the expected minimum and maximum value for columnar to equiaxed transition.

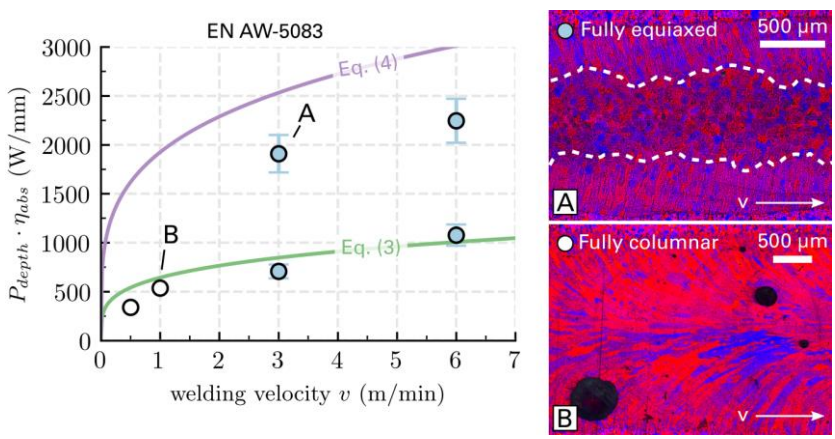

Fig. 4. Experimental results of EN AW-5083 are depicted for different absorbed power per unit depths and welding velocities. A circle filled with white indicates a fully columnar dendritic grain structure and circle filled with blue indicates a fully equiaxed dendritic grain structure in the weld centre. The green and purple lines are calculated by Eq. (3) and Eq. (4). They represent the expected minimum and maximum value for columnar to equiaxed transition.

Fig. 4 depicts the experimental results of EN AW-5083. The experimental results show an equiaxed dendritic grain structure for welding velocities v > 2 m/min even though the data point is close to the minimum value (green curve) according to Eq. (3). A fully columnar dendritic grain structure is observed for the velocity of v = 0.5 and 1 m/min.

In conclusion, the experimental data validates the proposed analytical approach for a wide range of processing parameters and aluminium alloys. The application of Eq. (1) enables to design the welding process for the reliable formation of an equiaxed dendritic grain structure.

4.2. Influence of cooling rate on the equiaxed dendritic grain size

According to Tang and Vollertsen, 2014 a finer grain structure leads to a higher hot cracking resistance. Furthermore, as it is known from casting, a high cooling rate decreases the grain size as shown by Easton and StJohn, 2008. This section relates the experimental measured equiaxed grain size of the conducted experiment with the calculated cooling rate.

The corresponding cooling rate

$$\dot{T} = 2\pi \cdot \left(T_{liq} - T_{amb}\right)^3 \cdot \lambda_{th} \cdot \rho_s \cdot c_p \cdot \frac{v^2}{P_{depth}^2 \cdot \eta_{abs}^2} \qquad (5)$$

for the different parameters was calculated according to Hagenlocher et al., 2019a. The required thermo-physical values are published by Ostermann, 2014.

Fig. 5 shows the equiaxed dendritic grain size as a function of the cooling rate. The data points with no equiaxed dendritic grain structure are displayed in Fig. 5 with an equiaxed dendritic grain size of d_{eqx} = 0 µm. The data points represent the mean, minimum and maximum measured grain size of one weld trial. The data shows a grain refinement in the weld grain structure with an increasing cooling rate. A high welding velocity combined with a low power per unit depth that still fulfils the criterion according to Eq. (1) leads to a fine grain structure.

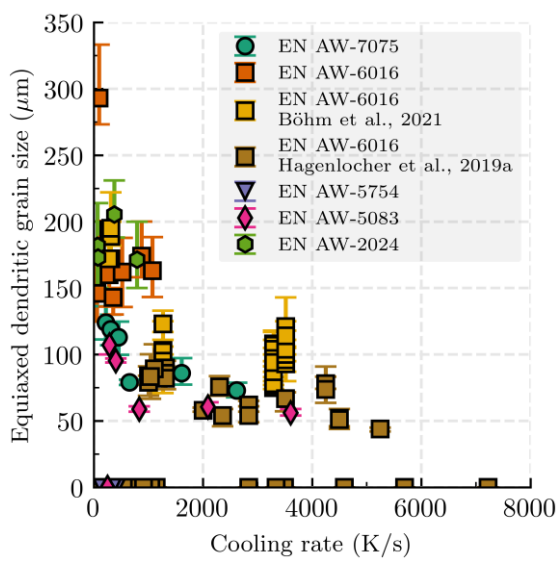

Fig. 5. The experimentally measured equiaxed dendritic grain size in the weld center for all conducted experiments and two literature values are related to their corresponding calculated cooling rate according to Eq. (5).

5. Summary

This study highlighted the analytical description for an equiaxed dendritic solidification for various aluminium alloys for full penetration laser beam welding. With the presented analytical approach, the process can be designed in order to reach the beneficial equiaxed dendritic grain structure. Furthermore, it was found that two conditions must be fulfilled for grain refinement in the weld seam. First, the absorbed power per unit depth must be high enough to reach the condition for the equiaxed solidification and second, the welding velocity must be high to increase the cooling rate.

Acknowledgements

This work was funded in parts by the Deutsche Forschungsgemeinschaft (DFG, German Research Foundation)—398552773.

References

Andersson J. O., Helander T., Höglund L., Shi P., Sundman B., 2002. Thermo-Calc & DICTRA, computational tools for materials science. Calphad: Computer Coupling of Phase Diagrams and Thermochemistry 26, pp 273–312. doi: 10.1016/S0364-5916(02)00037-8

Böhm C., Hagenlocher C., Wagner J., Graf T., Weihe S., 2021. Analytical Description of the Criterion for the Columnar-To-Equiaxed Transition During Laser Beam Welding of Aluminum Alloys. Metall Mater Trans A. doi: 10.1007/s11661-021-06238-0

Dantzig J., Rappaz M. (2016). Solidification, 2nd. EPFL Press

Easton M. A., StJohn D. H., 2008. Improved prediction of the grain size of aluminum alloys that includes the effect of cooling rate. Materials Science and Engineering: A 486, pp 8–13. doi: 10.1016/j.msea.2007.11.009

Gouffé A., 1945. Corrections d'ouverture des corps-noirs artificiels compte tenu des diffusions multiples internes. Rev. opt. 24, pp 1–7

Hagenlocher C., Fetzer F., Weller D., Weber R., Graf T., 2019a. Explicit analytical expressions for the influence of welding parameters on the grain structure of laser beam welds in aluminium alloys. Materials and Design 174, p 107791. doi: 10.1016/j.matdes.2019.107791

Hagenlocher C., Weller D., Weber R., Graf T., 2019b. Reduction of the hot cracking susceptibility of laser beam welds in AlMgSi alloys by increasing the number of grain boundaries. Science and Technology of Welding and Joining 24, pp 313–319. doi: 10.1080/13621718.2018.1534775

Hügel H., Graf T. (2014). Laser in der Fertigung, 3rd edn. Vieweg+Teubner, Wiesbaden

Hunt J. D., 1984. Steady state columnar and equiaxed growth of dendrites and eutectic. Materials Science and Engineering 65, pp 75–83. doi: 10.1016/0025-5416(84)90201-5

Ostermann F. (2014). Anwendungstechnologie Aluminium, 3. Auflage. Springer Vieweg

Rosenthal D., 1941. Mathematical theory of heat distribution during welding and cutting. Welding Journal 20, pp 220–234

Schempp P., Rethmeier M., 2015. Understanding grain refinement in aluminium welding: Henry Granjon Prize 2015 winner category B: materials behaviour and weldability. Welding in the World 59, pp 767–784. doi: 10.1007/s40194-015-0251-2

Tang Z., Vollertsen F., 2014. Influence of grain refinement on hot cracking in laser welding of aluminum. Welding in the World 58, pp 355–366. doi: 10.1007/s40194-014-0121-3